

Accepted Manuscript

Tissue Transport Affects How Treatment Scheduling Increases the Efficacy of Chemotherapeutic Drugs

Dan E. Ganz , Briana Sexton-Stallone , Emily L. Brackett ,
Neil S. Forbes

PII: S0022-5193(17)30486-1
DOI: [10.1016/j.jtbi.2017.10.022](https://doi.org/10.1016/j.jtbi.2017.10.022)
Reference: YJTBI 9246



To appear in: *Journal of Theoretical Biology*

Received date: 18 August 2016
Revised date: 17 October 2017
Accepted date: 20 October 2017

Please cite this article as: Dan E. Ganz , Briana Sexton-Stallone , Emily L. Brackett , Neil S. Forbes ,
Tissue Transport Affects How Treatment Scheduling Increases the Efficacy of Chemotherapeutic Drugs
, *Journal of Theoretical Biology* (2017), doi: [10.1016/j.jtbi.2017.10.022](https://doi.org/10.1016/j.jtbi.2017.10.022)

This is a PDF file of an unedited manuscript that has been accepted for publication. As a service to our customers we are providing this early version of the manuscript. The manuscript will undergo copyediting, typesetting, and review of the resulting proof before it is published in its final form. Please note that during the production process errors may be discovered which could affect the content, and all legal disclaimers that apply to the journal pertain.

Highlights

- A tissue-transport model was developed to optimize chemotherapeutic schedules
- Increasing doses is most effective for drugs with intermediary cell binding rates
- Strong and weak binding drugs do not benefit as much from increasing doses
- Many doses are best for drugs with fast diffusivity and weak cell binding
- One dose is best for drugs with slow diffusivity or strong cell binding

Tissue Transport Affects How Treatment Scheduling Increases the Efficacy of Chemotherapeutic Drugs

Dan E. Ganz¹, Briana Sexton-Stallone¹, Emily L. Brackett¹, Neil S. Forbes^{1,*}

¹Department of Chemical Engineering
University of Massachusetts, Amherst
Amherst, MA, USA

*Corresponding author

Keywords: Chemotherapy, optimal treatment schedule, retention, tissue transport model, diffusion, cell binding, pharmacokinetics

Correspondence to:
Professor Neil S Forbes
Chemical Engineering
University of Massachusetts Amherst
159 Goessmann Laboratory
686 North Pleasant St.
Amherst, Massachusetts 01003, USA
Email: forbes@umass.edu
Tel.: +1 413 577 0132
Fax: +1 413 545 1647

Abstract

A method to predict the effect of tissue transport on the scheduling of chemotherapeutic treatment could increase efficacy. Many drugs with desirable pharmacokinetic properties fail *in vivo* due to poor transport through tissue. To predict the effect of treatment schedule on drug efficacy we developed an *in silico* method that integrates diffusion through tissue and cell binding into a pharmacokinetic model. The model was evaluated with an array of theoretical drugs that had different rates of diffusivity, binding, and clearance. The efficacy of each drug, quantified as the fraction of cells killed, was calculated for twenty dosage schedules. Simulations showed that efficacy strongly depended on tissue transport, with a range of 0.00 to 99.99%, despite each drug having equal plasma areas under the curve (AUC). For most drugs, schedules that increased exposure also increased efficacy. Drugs with fast clearance benefited the most from increasing the number of doses and was most effective for those with intermediary binding. All drugs with slow diffusivity were ineffective. For a subset of drugs, increasing the number of doses decreased efficacy. This phenomenon was unexpected because, when considering uptake into tissue, sustained plasma levels from multiple doses are generally assumed to be more effective. This counterintuitive decrease in efficacy was caused by drug retention within tumor tissue. These results established a set of rules that suggests how transport parameters affect the efficacy of drugs at different schedules. The two most predominant rules are (1) multiple doses improve efficacy for drugs with fast clearance, fast diffusivity and low to intermediate cell binding; and (2) one dose is most effective for drugs with slow clearance, slow diffusivity or strong cell binding. Understanding the role of tissue transport when determining drug treatment schedules would improve the outcome of preclinical animal experiments and early clinical trials.

Introduction

Predicting an optimal dosing regimen for a chemotherapeutic is essential for maximizing effectiveness. When investigating new drugs, dosage schedules are estimated late in the evaluation process, during preclinical animal studies and phase I clinical trials (Le Tourneau et al., 2009). This can be problematic because drugs that have promising efficacy *in vitro* can fail to be effective *in vivo*. Using the correct schedule has the potential to improve *in vivo* efficacy. One set of mechanisms that affects performance in living systems is transport within tumor tissue (Toley et al., 2013). An optimized treatment schedule could overcome unfavorable transport properties. A mathematical model that predicts response of *in vivo* tumor tissue to drugs with a given set of transport properties would define the optimal schedule and improve drug performance before direct evaluation. Optimizing treatment schedules would also increase the efficacy of existing therapies.

In the absence of predictive models, the determination of dosage schedules begins with preclinical animal experiments, which are used to determine the efficacy and lethal dose (LD) of potential drugs (Le Tourneau et al., 2009). Drugs that are efficacious and have manageable side effects move on to clinical trials. One goal of a phase I trial is to determine the maximum tolerated dose (MTD), which is determined by incrementally escalating the dose until dose-limiting toxicities are observed (He et al., 2006; Korn et al., 1994). The recommended dose for Phase II trials is set at the MTD or one dose lower than the MTD. Treatment schedules are designed based on drugs with similar toxicity levels (Le Tourneau et al., 2009).

Mathematical modeling could establish optimal therapeutic strategies prior to clinical trials. It has been known for some time that the time integral of the drug concentration in the plasma, or the area under the curve (AUC), is an effective predictor of efficacy (Nagai and Ogata, 1997). To achieve a given AUC, several treatment schedules are possible, including a single bolus injection, several intermittent boluses, or continuous infusion (Carlson and Sikic, 1983). As a strategy, using many small doses to maintain the AUC is counter to the classic “more is better” approach of dosing with the MTD (Takimoto, 2009). Single large doses may be necessary when the dosage windows is small and may not be as effective for modern targeted drugs with less toxicity (Takimoto, 2009). This strategy would be particularly effective if coupled with a mathematical prediction of plasma clearance (Poulin and Theil, 2002a; Poulin and Theil, 2002b).

Having favorable transport properties is an essential characteristic of a successful treatment of solid tumors (Lin and Lu, 1997; Minchinton and Tannock, 2006; Tredan et al., 2007). Even with desirable efficacy against cells, drugs can fail *in vivo* due to poor tissue-level transport. Transport is important because of the physiology of solid tumors (Figure 1). Chemotherapy is typically administered as an IV bolus, and it reaches cancer cells by diffusing out of vasculature and through interstitial tumor tissue (Figure 1) (Lankelma et al., 1999). In tumors, drugs bind and are released from tumor cells (Bryn and Dolch, 1978; Lankelma, 2002). The rate of cell death is dependent on the local drug concentration. Drugs that do not effectively penetrate tissue cannot clear the regions that are far from the vasculature, despite being able to kill cells in culture (El-Kareh and Secomb, 1997; Venkatasubramanian et al., 2008). A drug’s ability to penetrate tumor tissue is determined by its diffusivity, the rate of binding to cells and the systemic rate of clearance (Toley et al., 2013).

Several models have been reported that predict treatment schedules based on drug parameters. By looking at the cytotoxicity of several drugs, a pharmacodynamic model determined that the effect on cells was heavily dependent on the time of exposure (Levasseur et al., 1998). A model of doxorubicin diffusion and uptake showed that extending infusion times and fractionating large doses would increase anti-tumor activity while reducing cardiotoxicity (Eikenberry, 2009). A model of cisplatin pharmacodynamics showed that predictions of cell survival based on AUC heavily depend on exposure time (El-Kareh and Secomb, 2003). A similar model, designed to predict response to combinations of chemotherapeutic drugs, showed that cell death was the result of additive damage by different mechanisms (Jones et al., 2014). Inclusion of saturation into the expression for cell response better matched experimental observations of plateaus in cell survival at high drug concentrations than models lacking these terms. A technique called model predictive control (MPC) was used to predict optimal schedules for therapy in the absence of complete time-dependent data, which would enable better dosing for individual patients (Chen et al., 2012). A meta-model of paclitaxel response showed that dose-dense chemotherapy yields better overall and disease-free survival (Lu et al., 2014). Many of these drug-efficacy models incorporated cell death kinetics and systemic pharmacokinetics, but did not explicitly include tissue-level transport.

To predict the effect of transport on the efficacy of different treatment schedules, we created a drug efficacy model that incorporates three critical phenomena: diffusion, cell binding and clearance. To evaluate this model, an array of theoretical drugs were generated that span possible values for the transport parameters and optimal treatment schedules were determined for each.

For all of the drugs and schedules, the plasma area under the curve (AUC) was kept the same. This meant that all measured differences were due to the effects of tissue transport. Efficacy was quantified as the total number of cells killed. Treatment schedules were evaluated by varying the number of doses and determining efficacy. From these calculations, general rules were established to relate transport parameters to schedule type. The mechanisms connecting drug parameters to optimal schedule was determined by quantifying the location and timing of drug delivery within tumor tissues. Ultimately, this computational tool and these results could enable better prediction of which treatment schedules are better for which drugs and which properties should be built into newly synthesized drugs to optimize their performance.

1. Methods

1.1. Model Formulation

Mass transport in tumor tissue was modeled with three simultaneous time-dependent partial differential equations that balance free drug (C), drug bound to cells (B), and the local fraction of viable cancer cells (N).

$$\frac{\partial C}{\partial t} = D \frac{\partial^2 C}{\partial x^2} - k_{on}C + k_{off}B \quad (1)$$

$$\frac{\partial B}{\partial t} = k_{on}C - k_{off}B \quad (2)$$

$$\frac{\partial N}{\partial t} = -\alpha \left(\frac{L^n}{K_d + L^n} \right) N \quad (3)$$

In these equations, k_{on} is the kinetic on rate for drugs binding to cells (1/s), k_{off} is the rate constant of drug release from cells (1/s), α is the maximum rate of cell death (1/s), n is the Hill coefficient, L is the combined concentration of bound and free drug ($C + B$; μM), and K_d is the drug dissociation constant (μM). In Equation 1, the rate of change of the concentration of free

drug ($\partial C/\partial t$) is dependent upon diffusion through tissue, binding to tumor cells and release of bound drug (Figure 1). The rate of change of bound drug (Eq. 2), is dependent on free drug binding to tumor cells and its release. The rate of change of live cells (Eq. 3) depends on the drug's maximum rate of cell killing (α) and the concentration that saturates drug binding and cell killing (K_d). The model assumes a Hill coefficient of one. When the saturation fraction approaches unity ($L \gg K_d$), cells are killed at the maximum rate. This pharmacodynamic model assumes that the rate of cell killing is proportional to drug concentration but has an upper limit (cannot be infinite) at high drug concentrations. This model has been used previously to describe cell death (Toley et al., 2013; Venkatasubramanian et al., 2008; Venkatasubramanian et al., 2010) and is based on dose-escalation experiments (Au et al., 1998; Erlichman and Vidgen, 1984; Kufe and Major, 1981; Mantovani, 1977; Ueda et al., 1997). The model assumes that free (C) and bound (B) drugs are present in both the intracellular and extracellular compartments and that both contribute to cell death. The effects of the cell cycle were not included because we previously showed that its inclusion did not improve predictions in models that also included diffusion through tissue (Venkatasubramanian et al., 2008).

Before drug was administered, the concentrations of free and bound drug was zero throughout the tissue, and all cells were alive.

$$@ t = 0 \quad C = 0, B = 0, N = 1 \quad (4)$$

The distal edge of the tissue ($x = L$) was assumed to be between blood vessels, which created a no-flux, Neumann boundary condition.

$$@ x = L \quad \frac{dC}{dx} = 0 \quad (5)$$

At the proximal edge of the tissue ($x = 0$), the drug concentration dropped with half-life $t_{1/2}$.

$$@ x = 0 \quad C = C_0 \exp\left(\frac{-\ln 2}{t_{1/2}} t\right) \quad (6)$$

This effective plasma concentration was initially given by C_0 . It differs from a measured plasma concentration by the effects of transport through endothelial cells and partitioning from the plasma into tissue. For experimental drugs, C_0 and $t_{1/2}$ could be adjusted to account for these effects. For theoretical drugs, these adjustments are not available and the most appropriate comparison is between drugs with equivalent effective plasma concentrations.

Treatment schedules were defined by the number of doses (m), where $m \in M$ and $M = (1, \dots, 20)$. With multiple doses ($m > 1$), the effective plasma concentration was given by the sum of exponentially decreasing clearance functions that started at increasing time increments.

$$@ x = 0 \quad C = \sum_{i=0}^{m-1} \frac{C_0}{m} H\left(t - \frac{iT}{m}\right) \exp\left[\frac{-\ln 2}{t_{1/2}} \left(t - \frac{iT}{m}\right)\right] \quad (7)$$

The time to dose i , was given by iT/m , where T was the total drug treatment time. The Heaviside step function, $H(t - iT/m)$, started each dose i at equally spaced intervals of T/m . The resultant concentration from each dose decreased exponentially with a delay of iT/m and with a half-life of $t_{1/2}$, similar to a single dose. The initial concentration of each dose (C_0/m) was scaled by the number of doses to maintain a constant total dose of drug for all regimens. It was assumed that drugs were not metabolized within the tumor tissue. This is reasonable for most small molecule drugs with the exception of a few small molecules (e.g. tirapazine) (Pruijn et al., 2005) and some large proteins and nanoparticle drugs (Vasalou et al., 2015).

To simplify the notation, equations (1) and (2) were nondimensionalized.

$$\frac{\partial \bar{C}}{\partial \bar{t}} = \frac{\partial^2 \bar{C}}{\partial \bar{x}^2} - Q\bar{C} + (Q/R)\bar{B} \quad (8)$$

$$\frac{\partial \bar{B}}{\partial \bar{t}} = Q\bar{C} - (Q/R)\bar{B} \quad (9)$$

In these equations, dimensionless concentrations were normalized by the initial effective plasma concentration ($\bar{C} = C/C_0$ and $\bar{B} = B/C_0$); distance was normalized by tissue thickness ($\bar{x} = x/L$); and time was normalized by the characteristic diffusion time ($\bar{t} = tD/L^2$). Dimensionless binding (Q) was the ratio of the kinetic on rate to the diffusivity ($Q = k_{on}L^2/D$). The dimensionless binding constant (R) was the ratio of the kinetic on rate to the kinetic off rate (k_{on}/k_{off}) and defines how tightly a drug binds to cells. Previous perturbation analysis showed that the model was a strong function of the binding constant, $R = k_{on}/k_{off}$, and insensitive to k_{on} . (Toley et al., 2013)

1.2. Data Analysis

An array of theoretical drugs was created with different values for diffusivity (D), binding (R), and clearance (pharmacokinetic half-life, $t_{1/2}$). The ranges for diffusivity and binding were created to encompass most possible physical values (Table 1). Values for these variable parameters were derived from the measured values for doxorubicin, because measurements have not been made for most clinical chemotherapeutic drugs. For doxorubicin, diffusivity is $2.9 \times 10^{-11} \text{ m}^2/\text{s}$, the binding constant is 48, and the half-life is 0.2 hours (Toley et al., 2013). Several parameters were kept constant for all theoretical drugs, and their values were matched to those of doxorubicin (Table 2). These static parameters included total dose administered (C_0), the maximum rate of cell death (α) and the dissociation (saturation) constant (K_d).

The system of equations were solved for each theoretical drug using finite elements in Matlab (*Mathworks*, Natick, MA). Simulations were repeated for each drug for all treatment schedules consisting of 1 to 20 doses. The outputs of the simulations were the local fraction of viable cells $[N(k,m,t,x)]$ and the concentrations of free and bound drug $[C(k,m,t,x)]$ and $[B(k,m,t,x)]$ as functions of drug (k , with properties D , R and $t^{1/2}$), dosage schedule (m), time (t), and position within the tissue (x). The overall fraction of killed cells (Fk) for each drug (k) at each dosage schedule (m) was the local fraction of cells killed averaged over the length of the tissue.

$$Fk_{k,m}(t) = 1 - \frac{1}{L} \int_{x=0}^{x=L} N(k,m,t,x) \quad (10)$$

The efficacy ($Eff_{k,m}$) of each drug was defined as the overall fraction of cells killed at the end of the treatment period, T .

$$Eff_{k,m} = Fk_{k,m}(t = T) \quad (11)$$

Three parameters were created to analyze efficacy and determine an optimal treatment schedule: maximum efficacy (MxE), multiple-dose improvement (MDI), and optimal treatment schedule (OpD). These parameters were determined for each of the theoretical drugs from the efficacy (Eff), after treatment with all of the possible treatment schedules. Maximum efficacy (MxE_k) of drug k was defined as the maximum efficacy over all dosages.

$$MxE_k = \max\{Eff_{k,m} | m = 1, \dots, 20\} \quad (12)$$

Multiple-dose improvement (MDI) was defined as the fraction of cells killed by 20 doses subtracted from the fraction killed by 1 dose.

$$MDI_k = Eff_{k,20} - Eff_{k,1} \quad (13)$$

This parameter indicates whether implementation of more than one dose would improve efficacy. When MDI is negative, increasing doses decreased efficacy and one dose is

advantageous. The optimal treatment schedule (OpD) is the least number of doses at which there existed a 2% difference from the maximum efficacy.

$$OpD_k = \min\{m | MxE_k - Eff_{k,m} < 0.02\} \quad (14)$$

Exposure of the tissue to drug k was estimated with the distal drug exposure ($DDE_{k,m}$). This scalar parameter is the time average of the concentration at the distal end of tissue [$C_D(k, m, t) = C(k, m, t, x=L) + B(k, m, t, x=L)$].

$$DDE_{k,m} = \frac{1}{T} \int_{t=0}^{t=T} C_D dt \quad (15)$$

Values for $DDE_{k,m}$ were obtained by numerical integration over the full treatment time (T) using Simpson's rule. Both bound and free drug contributed to $DDE_{k,m}$. To more easily analyze $DDE_{k,m}$, it was normalized to the range $[0, 1]$ using the drug saturation constant.

$$DDE'_{k,m} = \frac{DDE_{k,m}}{K_m + DDE_{k,m}} \quad (16)$$

The effect of increasing doses was described by subtracting the normalized distal exposure after 1 dose from the exposure after 10 doses.

$$\Delta DDE'_k = DDE'_{k,10} - DDE'_{k,1} \quad (17)$$

Drug retention (Rt_k) in the tissue was defined as the integral of the difference between the distal (C_D) and proximal [$C_P(k, m, t) = C(k, m, t, x=0) + B(k, m, t, x=0)$] concentrations for one dose ($m = 1$). Only positive differences were included to exclusively capture instances where the concentration was greater at the distal end.

$$Rt_k = \frac{1}{C_P^0} \int_{t=0}^{t=T} \{C_D - C_P | C_D > C_P\} dt \quad (18)$$

Values were normalized by the initial concentration at the proximal end [$C_p^0(k, m) = C(k, m, t=0, x=0) + B(k, m, t=0, x=0)$]. Negative *MDI* values (*MDIn*) indicated drugs that decreased in performance with increased doses.

$$MDIn = |\{MDI | MDI < 0\}| \quad (19)$$

The average drug exposure was defined as the integral of the concentration across the length of the tissue at a given time, normalized by the length of the tissue (L).

$$C_{k,m}^{ave}(t) = \frac{1}{L} \int_{x=0}^{x=L} [C(k, m, t, x) + B(k, m, t, x)] dx \quad (20)$$

Both bound and free drug contributed to C^{ave} . The effect of drug washout was quantified using the average drug exposure at half of the drug treatment time, after one dose.

$$C_k^{hf} = C_{k,1}^{ave}(t = T/2) \quad (21)$$

2. Results

Transport of chemotherapeutic drugs in tumors

When a chemotherapeutic drug is administered, it diffuses in and out of tissue, and kills cells while it is present (Figures 1, 2). The example drug (**Drug A**) in Figure 2 has transport properties similar to doxorubicin, with a diffusivity (D) of 10^{-10} m²/s, a cell binding constant (R) of 10^0 , and a half-life ($t_{1/2}$) of 0.5 hours. The drug concentration in the proximal tissue bordering the blood vessel drops with a rate equal to the systemic clearance rate (Figure 2A). It takes time for the drug to diffuse to the distal end of the tissue. At the time of administration, the concentration in this region is zero and increases until it reaches a maximum. In the distal region, the drug concentration decreases more slowly because it has to diffuse farther to the blood stream. This retention increases the efficacy of the drug because it increases the time that cells are exposed. In

combination, clearance and retention affected the average drug concentration across the whole tissue (Figure 2B). The drug killed cells until it was cleared from the blood and the tissue. By 5.0 hours the average drug concentration had dropped to 3.8% of its initial value and 87% of the final number of cells had been killed (Figure 2B).

Treatment schedules

The effect of different dosing regimens was implemented by increasing the number of doses (m) within a 72-hour period (Figure 3). Mathematically, dose schedules were incorporated into the model by adjusting the effective concentration of the drug in the plasma, which gives the boundary condition at $x = 0$ (Eq. 7). A two-dose treatment schedule consisted of two influxes of drug followed by exponential clearance (Figure 3A). Similarly, a 20-dose treatment schedule had 20 influxes (Figure 3B). For each regimen, the total amount of administered drug was kept constant. This criterion reduced the per-dose concentration (C_0/M) as the number of doses increased. For example, the individual-dose concentration was ten times greater for a 2-dose regimen (Figure 3A) than for a 20-dose regimen (Figure 3B). With two doses at a slower clearance rate (i.e. a 15 h half-life), the concentration almost returns to zero between doses (Figure 3C). However, with 20 doses, the short time between doses did not allow it to decrease much and the effective plasma concentration increased with time (Figure 3D). For drugs with slow clearance rates and schedules with many doses, the concentration approached a maximum value, similar to constant infusion. For a clearance rate of 15 hours and a schedule of 20 doses the effective plasma concentration approached a normalized value of 0.62. These half-life values were chosen, because, with many doses, the plasma concentration returned to zero after each dose for a half-life of 0.5 hours (Figure 3B), but did not for a half-life of 15 hours (Figure 3D).

These values for a terminal half-life (0.5 – 15 hr) are small compared to most small-molecule drugs, but were investigated because they show the greatest effects of diffusivity and binding.

Effect of multiple doses on cell viability

Increasing the number of doses had different effects on cell death in tumor tissue depending on the transport parameters of the drug (Figure 4). For a drug with moderate diffusivity of $10^{-8} \text{ m}^2/\text{s}$, a binding constant of 10^{-2} , and a half-life of 0.5 hours (**Drug B**), increasing the number of doses increased the efficacy and the number of cells killed (Figure 4A). However, increasing the number of doses for a drug with a lower diffusivity of $10^{-12} \text{ m}^2/\text{s}$, a higher binding constant of 10^2 and the same clearance (**Drug C**), decreases efficacy (Figure 4B). For **Drug B**, the biggest gains in efficacy were after the addition of the first few doses. Similarly, for **Drug C**, the majority of the decrease in efficacy occurred after adding the first few doses. After four doses, the effect flattened and more doses did not affect the fraction of killed cells.

To quantify the effect of dosage schedule on drug efficacy three parameters were determined for all drugs: multiple-dose improvement (*MDI*), maximum efficacy (*MxE*) and optimum schedule (*OpD*). *MDI* is the difference between the fraction of cells killed by 20 and 1 doses. For example, the drug with moderate diffusivity in Figure 4A (**Drug B**) had an *MDI* of 0.42. The slower diffusing drug (**Drug C**) had an *MDI* of -0.02. This parameter indicates whether a regimen with more doses increased or decreased efficacy. Maximum efficacy was the greatest fraction of cells killed over all schedules. Optimal schedule is the number of doses that produces the maximum effect. For **Drug B**, the maximum was 0.62 at 20 doses and for **Drug C** the maximum was 0.23 at one dose.

Effect of transport and dosing on efficacy

To systematically determine how transport parameters affected efficacy and optimum treatment schedules, an array of theoretical drugs was created (Figure 5). These drugs had different transport and delivery parameters: diffusivity (D), cell binding (R), and systemic clearance ($t_{1/2}$). The ranges for D and R were 10^{-15} to 10^{-7} m²/s and 10^{-4} to 10^4 . Three values for $t_{1/2}$ were tested: 0.5, 5 and 15 hours. The range of diffusivities was chosen to be larger than the range from small metabolites (10^{-9} m²/s) to nanoparticle drugs (10^{-13} m²/s) to incorporate diffusion values for all possible experimental drugs. These ranges span the diffusivities and binding constants of some commonly investigated drugs, e.g. tirapazine variants ($D = 2.70 - 21.0 \times 10^{-10}$ m²/s) (Pruijn et al., 2005); nanoparticle-bound drugs ($D = 1.3 \times 10^{-11}$ m²/s, $R = 10$) (Vasalou et al., 2015); and adriamycin ($D = 2.78 \times 10^{-9}$ m²/s, $R=3$) (Eikenberry, 2009).

The efficacy of drugs with fast clearance ($t_{1/2} = 0.5$ h) were highly dependent on tissue transport properties (Figure 5). For all of these drugs and schedules, the plasma AUC was constant. Of these drugs, the efficacy of some were affected by dose, some were always effective, and others were ineffective regardless of schedule. In the group of drugs with fast clearance, the greatest efficacy was for those with high diffusivities and high binding constants (Figure 5A, *upper right*). (Drugs with slower clearance were less dependent on transport parameters and are described in more detail below.) Drugs with low binding constants ($R < 10^2$) and high diffusivities ($D > 10^{-10}$ m²/s) were not as effective (Figure 5A, *lower right*) as those with higher binding constants. Across all binding constants, efficacy increased for drugs with higher

diffusivity. At low diffusivities ($D < 10^{-13} \text{ m}^2/\text{s}$), all drugs were ineffective regardless of binding constant and treatment schedule (Figure 5A, *left*).

For a subset of drugs, there was significant improvement in efficacy with treatment schedules of more than one dose (Figure 5B). The extent of improvement (*MDI*) depended on the drug's diffusivity and cell binding. At a half-life of 0.5 hours, increasing the number of doses did not increase the efficacy ($MDI \leq 0$) for all slow diffusing drugs with diffusivities less than $10^{-12} \text{ m}^2/\text{s}$. For a band of drugs with diffusivities between 10^{-9} and $10^{-13} \text{ m}^2/\text{s}$ and a binding constant greater than 10^0 , *MDI* was negative indicating decreased efficacy with increased number of doses. For faster diffusing drugs ($D \geq 10^{-10} \text{ m}^2/\text{s}$), *MDI* had an optimum with cell binding (R). Drugs with a binding constant between 10^{-1} and 10^1 had the greatest *MDI* indicating that increasing doses had the greatest effect. In this range, a treatment schedule with more than one dose improved efficacy the most ($0.39 \leq MDI \leq 0.64$). For strong binding drugs ($R \geq 10^1$) with fast diffusivity, extra doses had little effect. At low binding constants ($R \leq 10^{-1}$) the increase in efficacy with extra doses was less pronounced.

Optimum number of doses

A treatment schedule with more doses was beneficial for drugs with high diffusivity and low binding constants (Figure 5C). The optimum number of doses was the number of doses that produced the maximum efficacy (Figure 5A). For both slow diffusing ($D \leq 10^{-11} \text{ m}^2/\text{s}$) drugs and strongly binding ($R \geq 10^2$) drugs, one dose was most effective (Figure 5C). For fast diffusion drugs, with diffusivity greater than $10^{-11} \text{ m}^2/\text{s}$, the optimum number of doses was higher with lower binding constants. When cell binding was less than 10^0 , efficacy was greatest with

administration of the maximum number of doses. At intermediate binding constants ($10^1 \leq R \leq 10^3$), an intermediate number of doses ($2 \leq OpD \leq 14$) produced the optimum efficacy. At high binding ($R > 10^2$), increasing the number of doses did not measurably ($> 1\%$) increase efficacy and was not beneficial.

Drug classification

The array of theoretical drugs were arranged into five groups based on the effects of tissue transport on optimal dose (Figure 5D). Group I drugs have diffusivities less than 10^{-13} m²/s. In this group, diffusion was too low to be effective and increasing dosing did not improve performance. Group II drugs have moderate diffusivity between 10^{-9} and 10^{-13} m²/s and binding greater than 10^0 . These drugs performed best with a single dose. Increasing the number of doses was counterproductive and decreased overall efficacy. Drugs with high diffusivity ($D > 10^{-11}$ m²/s) and high binding ($R > 10^1$; Group III) were always effective. Increasing the number of doses in this region did not increase efficacy because a single dose killed almost all cells. At intermediate binding constants ($10^{-1} \leq R \leq 10^1$; Group IV), increasing the number of doses had the greatest effect, and an intermediate number of doses produced the optimum effect. At lower binding constants ($R < 10^{-1}$; Group V), the effect of increasing doses was less pronounced and the maximum number of doses was required to produce the greatest efficacy.

Increased exposure increased efficacy

For most drugs, those with higher exposure had higher efficacy. Similarly, when increasing the number of doses increased the total exposure, the efficacy increased (Figure 6). This effect was pronounced for theoretical **Drug D**, which has a diffusivity of 10^{-7} m²/s and a binding constant of

10^2 . The time profile of the drug concentration at the distal edge of the tissue captured the effect of penetration of this drug into the tissue (Figure 6A,B). When the number of doses was increased from 1 to 10, the efficacy improved from 0.485 to 0.993 (Figure 6C,D). When one dose was administered, tumor cell killing stopped (Figure 6C) as soon as the drug was cleared from the distal edge (Figure 6A). Multiple small doses were more effective (Figure 6D). With more doses, the concentration of drug at the distal edge was higher for a longer period of time (Figure 6B), which continued to kill cells throughout the treatment (Figure 6D). Although more drug was present at earlier times with a single dose, cell killing was close to its maximum rate. With a single dose, the concentration was higher than the saturation constant (K_d) and the excess drug provided no benefit. Having a greater dose at earlier times did not kill more cells.

An estimate of exposure was given by the Distal Drug Exposure (DDE), which is the integral of the drug concentration at the distal edge over treatment time (Figure 6E,F). Total exposure was controlled by penetration of the drug into tissue and its retention after clearance from the blood. The DDE parameter describes how long the drug is maintained at the distal end of the tumor tissue. To more easily visualize DDE , it was normalized to the range $[0, 1]$ using the drug saturation (dissociation) constant (K_d) and termed DDE' . For **Drug D**, increasing the number of doses from 1 to 10, increased DDE' from 0.850 and 0.994. There are similarities between DDE' (Figure 6E,F) and MxE (Figure 5A). When diffusivity was slow (Group I), both DDE' and MxE were low, regardless of schedule. When diffusivity was fast and binding was high (Group III), both DDE' and MxE were high. All drugs with poor exposure (Figure 6E,F) had poor efficacy (Figure 5A), regardless of schedule. Similarly, all drugs and schedules with positive distal exposure had positive efficacies.

The effect of treatment schedule on exposure was best visualized by the change in distal exposure between 1 and 10 doses, $\Delta DDE'$ (Figure 6G). The effect of diffusivity and binding on $\Delta DDE'$ are similar to the effect on MDI (Figure 5B). Drugs in Groups I and II had $\Delta DDE'$ values close to zero, matching MDI . In these regions, exposure was small for both 1 and 10 doses (Figure 6E,F), indicating that increasing the number of doses would not increase efficacy. Similarly, $\Delta DDE'$ for drugs in group III was small because DDE' was close to unity for both 1 and 10 doses (Figure 6E,F). The connection between efficacy and drug exposure was most prominent for drugs in Groups IV and V (Figure 6E-G). In groups IV and V there was a maximum in $\Delta DDE'$ with cell binding (Figure 6G), which matches the maximum in MDI over the same range (Figure 5B). This maximum indicates that the largest benefit of increasing doses for drugs in Group IV was because of increased exposure throughout the tissue. Most drugs that had increased efficacy with increased number of doses, also had an increase in exposure with more doses. Similarly, if efficacy did not increase, exposure did not increase.

Drugs with high retention perform best with single doses

Exposure did not completely explain all effects of increasing the number of doses. For a subset of theoretical drugs (Group II), increasing the number of doses *decreased* overall efficacy (Figure 7). This is the major difference between MDI and $\Delta DDE'$; for Group II drugs, MDI was negative, whereas $\Delta DDE'$ was positive for all drugs. This counterintuitive response of Group II drugs to increasing the number of doses was caused by retention in the tissue. Retention is the persistence of the drug within the tumor after it has cleared from the blood plasma. This phenomenon is greatest at intermediate diffusivities (Toley et al., 2013). At slow diffusivities,

drug cannot enter the tissue, and at high diffusivities, the tissue concentration matches the effective plasma concentration and is cleared from both at equal rates. At intermediate diffusivities, the drug diffuses into the tissue, but diffuses out slower than it is cleared from the blood. For example, after one dose, **Drug A** is present in the distal region for longer than in the proximal region (Figure 2A).

An example of a Group II drug with a negative *MDI* is **Drug C** ($D = 10^{-12} \text{ m}^2/\text{s}$, $R = 10^2$). For this drug, when the number of doses was increased from 1 to 20, the efficacy decreased (Figure 4B, 7A-D). After one large dose, the rate of killing was initially fast and slowed with time (Figure 7A). With twenty doses, the killing rate increased constantly, but did not reach the effect of one dose by 72 hours (Figure 7A). The difference between these two profiles produced a negative *MDI* (MDI_n , Figure 5B). The continued killing after clearance from the plasma was caused by the positive and substantial drug concentration in the tissue throughout the treatment (Figure 7B). After a one-dose treatment, the drug was quickly cleared from the proximal region (Figure 7C). With time, the drug appears at the distal end where it was retained for a longer time (Figure 7D). Because of retention in the tissue after one dose, the average concentration across the tissue (C^{ave}) remained high for the duration of treatment (Figure 7B). For comparison, the distal concentration of **Drug D**, which has a faster diffusion ($D = 10^{-7} \text{ m}^2/\text{s}$), dropped to zero after the drug was cleared from the plasma (Figure 6A). Therefore, the reason that the efficacies of drugs in Group II decrease with more doses is because 1 dose is more effective, not because 20 is less.

For each drug, retention (Rt) was defined as the integral of the difference between the concentration at the distal and proximal edge (Figure 7E). Differences were only included if greater than zero and values were normalized by the proximal concentration at $t = 0$. For drugs without retention, the value of Rt was zero (Figure 7E). For example, Rt for **Drug A** was 0.84. Over the range of D and R , drugs with high retention (Rt ; Figure 7E) mostly matched drugs with MDI (Figure 7F).

Effect of clearance

Increasing the number of doses had less effect on drugs with slower clearance rates (Figure 8). At higher half-lives of 5 and 15 hours, diffusivity had a greater influence on efficacy (MxE) than binding (Figure 8A,B) and MDI was almost independent of transport parameters (Figure 8C,D). Similar to fast clearing drugs (Figure 5), all slow diffusing drugs (Group I, $D < 10^{-13}$) were ineffective (Figure 8A,B). In the slower clearance range, cell binding did not have an effect. All fast diffusing drugs ($D > 10^{-13}$; Groups II - V) were effective at all doses (Figure 8A,B). For a half-life of five hours, MDI was greatest for Group V drugs ($D > 10^{-13} \text{ m}^2/\text{s}$, and $R < 10^{-1}$; Figure 8C). For these drugs, two doses was more effective than one (Figure 8E), because it increased overall exposure. For all other drugs with a half-life of five hours, one dose was optimum (Figure 8E). Drugs with intermediate diffusivity (10^{-14} to $10^{-12} \text{ m}^2/\text{s}$), had a negative MDI (Figure 8C). At a half-life of 15 hours, no improvement was seen with more than one dose for any drug (Figure 8D). MDI was small for all diffusivities and binding constants (Figure 8D). One dose was optimum for all drugs with a half-life of 15 hours (Figure 8F).

Increasing the number of doses had little effect on drugs with slow clearance because a single dose was often sufficient to attain the maximum effect (Figure 9). A slower clearance rate increased tissue exposure to the drug. After two doses of **Drug E** ($D = 10^{-7} \text{ m}^2/\text{s}$; $R = 10^0$) with $t_{1/2} = 0.5 \text{ h}$, the concentration at the distal end of the tissue spiked immediately after each dose then diminished quickly as the drug cleared from the system (Figure 9A). After treatment with a similar drug with the same diffusion and (D) and binding (R), but slower clearance ($t_{1/2} = 5 \text{ h}$), the concentration in the distal region diminished more slowly (Figure 9B). This increase in exposure throughout the tissue lead to increased efficacy for the drug with slow clearance (Figure 9D) compared to the drug with faster clearance (Figure 9C). Because the slow-clearing drug was present throughout the period between doses (Figure 9B), it killed almost all of the cells by the time the second dose arrived (Figure 9D). The second dose, therefore, did not have much of an effect on the overall efficacy. Because one or two doses were so much more effective for drugs with slow clearance, adding more doses did not produce any benefit.

3. Discussion

Incorporating information about drug transport in tumor tissue is critical when determining dosage schedules. All of the transport parameters (D , R and $t_{1/2}$) affected dosage schedules differently. The systemic clearance rate had a large effect on schedule, as expected. Drugs that cleared slowly did not benefit from increasing the number of doses (Figures 8,9). At faster clearance rates, the effects were more complicated. For all drugs, slow diffusion prevented drugs from killing cells (Figures 5,8). When diffusivity was greater, slow clearing drugs were effective at all doses. For fast clearing drugs, the effect of increasing doses depended on cell binding and most improvement was seen at intermediate binding.

The model showed that local exposure time was the primary predictor of efficacy (Figure 6). The inclusion of tissue transport into the mathematical model showed that tissue exposure (Figure 6) is different from plasma area under the curve (AUC). For all drugs examined here, AUC was equal. The difference in efficacy was caused by tissue transport. An optimal treatment schedule would increase exposure, regardless of AUC, and improve efficacy.

An important phenomenon was retention of the drug in the tissue after clearance from the plasma (Figures 2,7). Retention increased the efficacy of some drugs beyond what would have been predicted by penetration alone. The importance of retention in tissue has been shown experimentally to be critical for some cancer drugs (Toley et al., 2013). However, retention also had a confounding, non-intuitive effect on the optimal dosage schedule. For moderately diffusing drugs, increasing the number of doses decreased efficacy (Figure 7). This occurred because, for these drugs, one large dose was retained within the tissue and outperformed multiple small treatments (Figure 7). Retention was the most unexpected observation made with the mathematical model. Without it, all drugs would perform best with more doses. Therefore, it is important to take this phenomenon into account to avoid an incorrect dosage schedule. This is especially important because retention has the greatest influence on drugs with moderate transport parameters, similar to those of established chemotherapeutics.

These results enabled the creation of a set of strategies for how to determine treatment schedules based on transport parameters (Table 3). Recommendations are based on drug group. Drugs in Group III with fast clearance, diffusivity and strong cell binding, are always effective and one

dose should be used because no improvement is seen with increased doses. For weak binding drugs in Group V, more doses always increases efficacy and the most doses possible should be used. Optimization is required for drugs with intermediate cell binding in Group IV. Experiments should be performed to determine how many doses produce the greatest effect. Experiments are important for this group because low doses may be less effective than predicted due to DNA repair. Similarly, the maximum tolerated dose may be greater for schedules with many small doses, which would enable use of higher concentrations and more effective killing.

Special care should be taken when determining dosage schedules for drugs in Group II with intermediate diffusivity. When the clearance rate is slow or fast, increasing the number of doses counter-intuitively decreases the efficacy of the drug. Multiple-dose strategies should be avoided and single doses favored.

The ubiquitous ineffectiveness of all slow diffusing drugs (Group I), regardless of clearance rate, highlights the importance of measuring the transport properties of cancer drugs. Regardless how efficiently a drug kills cancer cells, it will not be effective against solid tumors if it cannot penetrate. This observation is important for nanoparticle-bound drugs which could have diffusivities below the predicted cutoff of $10^{-13} \text{ m}^2/\text{s}$ (Vasalou et al., 2015). To date, the diffusivities of only a handful of drugs have been determined (Lankelma, 2002; Pruijn et al., 2005; Toley et al., 2013; Vasalou et al., 2015), including those that target tumor hypoxia (Hicks et al., 2006; Kyle and Minchinton, 1999). One method to measure diffusivity and cell binding is in a microfluidic device that contains a three-dimensional cell mass of cancer cells (Walsh et al., 2009). Such a device is capable of measuring all of the parameters (e.g. D and R) used in the

mathematical model described here. Cells are grown in cuboid chambers, similar to the geometry of the model, and drugs are supplied through a bordering flow channel. Microscopic measurement of drug concentration as a function of space and time can be fit to the transport model (Toley et al., 2013). Knowing that drugs will fail due to poor transport would prevent unnecessary animal trials.

The model performed very well at predicting the dosage schedule of a known chemotherapeutic. Doxorubicin currently has a 12-dose treatment schedule over a 72 hour period (Alley et al., 2004). The tissue-transport model predicted that six doses would be optimal, when this was defined as the number doses for which the efficacy was within 1% of the 20-dose schedule. When this definition was tightened to be 0.2% of the 20-dose schedule, the model predicted a 12-dose schedule. This model accurately predicted that doxorubicin benefits from a treatment schedule with more than one dose and has an *MDI* of 0.11.

Care should be taken quantitatively interpreting these results for all chemotherapeutics. The simulations assumed that the theoretical drugs (1) are delivered intravenously, (2) bind to cells reversibly, and (3) kill cells according to the Hill equation. If similar simulations were performed with drugs that irreversibly bind cells (e.g. DNA alkylating agents or suicide inhibitors of tyrosine-kinase inhibitors), the results would be quantitatively different. These drugs would not release from cells after penetration, which would greatly increase the effect of retention. Similarly, oral delivery (an alternative to assumption #1) would change the plasma concentration profile by increasing the absorption phase and would decrease the efficacy of repeat dosing. More complex mechanisms of drug killing (e.g. cell-cycle dependence or damage repair

enzymes) could decrease the predicted efficacy of the drugs. Although inclusion of alternate assumptions would affect the quantitative results, it would not change the overall insight provided by the model that transport plays a significant role in the efficacy of drugs and affects which treatment schedules are superior.

The rules established by the results presented here will help guide future animal and clinical trials. Often dosage schedules are established with the idea that more is better (Takimoto, 2009). These rules demonstrate that for some drugs every effort should be made to supply the greatest number of doses, whereas for others increasing the number of doses has no gain and may be detrimental. Depending on the drug, administering the drug with a delivery device could be more practical than many small doses and would have the same therapeutic effect. These conclusions are important for drugs with short terminal half-lives, as investigated here. For drugs with slow clearance, the limitation of slow diffusivity is important, but binding may play less of a role. Measuring transport parameters of experimental drugs would improve the efficacy of chemotherapy by better predicting optimal dosage schedules prior to trials. Incorporating mass transport into PK/PD models will improve the accuracy of prediction and will decrease experimental time, decrease costs, and increase treatment schedule efficacy.

Acknowledgements

We gratefully acknowledge financial support from the National Science Foundation (Grant No. 1159689).

References

- Alley, M., Hollingshead, M., Dykes, D., Waud, W., 2004. Human Tumor Xenograft Models in NCI Drug Development. In: Teicher, B. A., Andrews, P. A., Eds.), *Anticancer Drug Development Guide; Preclinical Screening, Clinical Trials, and Approval*. Humana Press, New York, pp. 125-152.
- Au, J. L. S., Li, D., Gan, Y. B., Gao, X., Johnson, A. L., Johnston, J., Millenbaugh, N. J., Jang, S. H., Kuh, H. J., Chen, C. T., Wientjes, M. G., 1998. Pharmacodynamics of immediate and delayed effects of paclitaxel: Role of slow apoptosis and intracellular drug retention. *Cancer Research* 58, 2141-2148.
- Bryn, S. R., Dolch, G. D., 1978. Analysis of binding of daunorubicin and doxorubicin to DNA using computerized curve-fitting procedures. *Journal of pharmaceutical sciences* 67, 688-93.
- Carlson, R. W., Sikic, B. I., 1983. Continuous infusion or bolus injection in cancer chemotherapy. *Annals of internal medicine* 99, 823-33.
- Chen, T., Kirkby, N. F., Jena, R., 2012. Optimal dosing of cancer chemotherapy using model predictive control and moving horizon state/parameter estimation. *Computer methods and programs in biomedicine* 108, 973-83, doi:10.1016/j.cmpb.2012.05.011.
- Eikenberry, S., 2009. A tumor cord model for Doxorubicin delivery and dose optimization in solid tumors. *Theoretical Biology and Medical Modelling* 6, doi:10.1186/1742-4682-6-16.
- El-Kareh, A. W., Secomb, T. W., 1997. Theoretical models for drug delivery to solid tumors. *Critical Reviews in Biomedical Engineering* 25, 503-571.
- El-Kareh, A. W., Secomb, T. W., 2003. A mathematical model for cisplatin cellular pharmacodynamics. *Neoplasia* 5, 161-169.
- Erlichman, C., Vidgen, D., 1984. Cyto-toxicity of adriamycin in MGH-U1 cells grown as monolayer-cultures, spheroids, and xenografts in immune-deprived mice. *Cancer Research* 44, 5369-5375.
- He, W., Liu, J., Binkowitz, B., Quan, H., 2006. A model-based approach in the estimation of the maximum tolerated dose in phase I cancer clinical trials. *Statistics in medicine* 25, 2027-42, doi:10.1002/sim.2334.
- Hicks, K. O., Pruijn, F. B., Secomb, T. W., Hay, M. P., Hsu, R., Brown, J. M., Denny, W. A., Dewhirst, M. W., Wilson, W. R., 2006. Use of three-dimensional tissue cultures to model extravascular transport and predict in vivo activity of hypoxia-targeted anticancer drugs. *J Natl Cancer Inst* 98, 1118-1128, doi:10.1093/jnci/djj306.
- Jones, L. B., Secomb, T. W., Dewhirst, M. W., El-Kareh, A. W., 2014. The additive damage model: A mathematical model for cellular responses to drug combinations. *Journal of Theoretical Biology* 357, 10-20, doi:10.1016/j.jtbi.2014.04.032.
- Korn, E. L., Midthune, D., Chen, T. T., Rubinstein, L. V., Christian, M. C., Simon, R. M., 1994. A comparison of two phase I trial designs. *Statistics in medicine* 13, 1799-806.
- Kufe, D. W., Major, P. P., 1981. 5-fluorouracil incorporation into human-breast carcinoma RNA correlates with cyto-toxicity. *Journal of Biological Chemistry* 256, 9802-9805.
- Kyle, A. H., Minchinton, A. I., 1999. Measurement of delivery and metabolism of tirapazamine to tumour tissue using the multilayered cell culture model. *Cancer Chemotherapy and Pharmacology* 43, 213-220, doi:10.1007/s002800050886.

- Lankelma, J., 2002. Tissue transport of anti-cancer drugs. *Current Pharmaceutical Design* 8, 1987-1993, doi:10.2174/1381612023393512.
- Lankelma, J., Dekker, H., Luque, R. F., Luykx, S., Hoekman, K., van der Valk, P., van Diest, P. J., Pinedo, H. M., 1999. Doxorubicin gradients in human breast cancer. *Clinical Cancer Research* 5, 1703-1707.
- Le Tourneau, C., Lee, J. J., Siu, L. L., 2009. Dose escalation methods in phase I cancer clinical trials. *Journal of the National Cancer Institute* 101, 708-20, doi:10.1093/jnci/djp079.
- Levasseur, L. M., Slocum, H. K., Rustum, Y. M., Greco, W. R., 1998. Modeling of the time-dependency of in vitro drug cytotoxicity and resistance. *Cancer Research* 58, 5749-5761.
- Lin, J. H., Lu, A. Y. H., 1997. Role of pharmacokinetics and metabolism in drug discovery and development. *Pharmacological Reviews* 49, 403-449.
- Lu, D., Joshi, A., Li, H., Zhang, N., Ren, M. M., Gao, Y., Wada, R., Jin, J. Y., 2014. Model-based meta-analysis for quantifying Paclitaxel dose response in cancer patients. *CPT: pharmacometrics & systems pharmacology* 3, e115, doi:10.1038/psp.2014.14.
- Mantovani, A., 1977. Invitro and invivo cytotoxicity of adriamycin and daunomycin for murine macrophages. *Cancer Research* 37, 815-820.
- Minchinton, A. I., Tannock, I. F., 2006. Drug penetration in solid tumours. *Nature reviews. Cancer* 6, 583-92, doi:10.1038/nrc1893.
- Nagai, N., Ogata, H., 1997. Quantitative relationship between pharmacokinetics of unchanged cisplatin and nephrotoxicity in rats: Importance of area under the concentration-time curve (AUC) as the major toxicodynamic determinant in vivo. *Cancer Chemotherapy and Pharmacology* 40, 11-18, doi:10.1007/s002800050618.
- Poulin, P., Theil, F. P., 2002a. Prediction of pharmacokinetics prior to in vivo studies. I. Mechanism-based prediction of volume of distribution. *Journal of pharmaceutical sciences* 91, 129-156, doi:10.1002/jps.10005.
- Poulin, P., Theil, F. P., 2002b. Prediction of pharmacokinetics prior to in vivo studies. II. Generic physiologically based pharmacokinetic models of drug disposition. *Journal of pharmaceutical sciences* 91, 1358-1370, doi:10.1002/jps.10128.
- Pruijn, F. B., Sturman, J. R., Liyanage, H. D. S., Hicks, K. O., Hay, M. P., Wilson, W. R., 2005. Extravascular transport of drugs in tumor tissue: Effect of lipophilicity on diffusion of tirapazamine analogues in multicellular layer cultures. *Journal of Medicinal Chemistry* 48, 1079-1087, doi:10.1021/jm049549p.
- Takimoto, C. H., 2009. Maximum tolerated dose: clinical endpoint for a bygone era? *Targeted Oncology* 4, 143-147, doi:10.1007/s11523-009-0108-y.
- Toley, B. J., Tropeano Lovatt, Z. G., Harrington, J. L., Forbes, N. S., 2013. Microfluidic technique to measure intratumoral transport and calculate drug efficacy shows that binding is essential for doxorubicin and release hampers Doxil. *Integrative biology* 5, 1184-96, doi:10.1039/c3ib40021b.
- Tredan, O., Galmarini, C. M., Patel, K., Tannock, I. F., 2007. Drug resistance and the solid tumor microenvironment. *J Natl Cancer Inst* 99, 1441-54.
- Ueda, M., Kumagai, K., Ueki, K., Inoki, C., Orino, I., Ueki, M., 1997. Growth inhibition and apoptotic cell death in uterine cervical carcinoma cells induced by 5-fluorouracil. *International Journal of Cancer* 71, 668-674, doi:10.1002/(sici)1097-0215(19970516)71:4<668::aid-ijc25>3.0.co;2-6.
- Vasalou, C., Helmlinger, G., Gomes, B., 2015. A Mechanistic Tumor Penetration Model to Guide Antibody Drug Conjugate Design. *Plos One* 10, doi:UNSP e0118977

10.1371/journal.pone.0118977.

Venkatasubramanian, R., Henson, M. A., Forbes, N. S., 2008. Integrating cell-cycle progression, drug penetration and energy metabolism to identify improved cancer therapeutic strategies. *Journal of theoretical biology* 253, 98-117, doi:10.1016/j.jtbi.2008.02.016.

Venkatasubramanian, R., Arenas, R. B., Henson, M. A., Forbes, N. S., 2010. Mechanistic modelling of dynamic MRI data predicts that tumour heterogeneity decreases therapeutic response. *British journal of cancer* 103, 486-97, doi:10.1038/sj.bjc.6605773.

Walsh, C. L., Babin, B. M., Kasinskas, R. W., Foster, J. a., McGarry, M. J., Forbes, N. S., 2009. A multipurpose microfluidic device designed to mimic microenvironment gradients and develop targeted cancer therapeutics. *Lab on a chip* 9, 545-54, doi:10.1039/b810571e.

Figure Captions

Figure 1. Mechanisms that control chemotherapeutic drug efficacy in tumors. The computational model of chemotherapeutic (*stars*) efficacy contains four main mechanisms: diffusion (D), binding (R), cytotoxicity (μ_D^{max}), and clearance ($t_{1/2}$). Drugs are delivered through the vasculature (*dark red*) and diffuse, with rate D , through tumor tissue (*orange*) made up of cells. After binding to cells with rate constant R , drugs cause cell death (*red star*) with maximum rate, μ_D^{max} . Drugs diffuse out of tissue with rate D and are cleared from the blood at rate $t_{1/2}$.

Figure 2. Drug transport in tumor tissue after a single dose. *A)* Transport of a theoretical drug (**Drug A**) with similar transport properties as doxorubicin ($D = 10^{-10} \text{ m}^2/\text{s}$; $B = 10^0$; and $t_{1/2} = 0.5 \text{ hr}$). Drug was introduced at a normalized concentration of one at time $t = 0 \text{ hr}$. Initially the proximal concentration (C_P) was greater than the distal concentration (C_D). With time, retention caused C_D to be greater than C_P . *B)* The average concentration in the tissue (C^{ave}) shows the combined effects of clearance and retention, which affected the proximal and distal concentrations in (*A*). The presence of drug killed cells (Fk) decreased until the drug was cleared from the system.

Figure 3. Effect of dosage schedule and clearance rate on effective plasma concentration. *A,B)* Effective plasma concentration for a drug with half-life of 0.5 hours and (*A*) 2-doses and (*B*) 10 doses. The amount of drug added per dose was ten times greater in A compared to B to keep the total drug administered constant. *C,D)* Effective plasma concentration for a drug with half-life of 15 hours and (*C*) 2-doses and (*D*) 10 doses.

Figure 4. Drug transport parameters affected how treatment schedule influenced efficacy.

A) For a drug (**Drug B**) with moderate diffusivity ($10^{-8} \text{ m}^2/\text{s}$) and binding (10^{-2}), increasing the number of doses increased efficacy. *B)* For a drug (**Drug C**) with lower diffusivity ($10^{-12} \text{ m}^2/\text{s}$) and higher binding (10^2), more doses decreased efficacy.

Figure 5. Effect of transport properties on efficacy. *A)* An array of theoretical drugs was evaluated over all dosage schedules. The maximum efficacy (MxE) across all schedules was highly dependent on diffusivity (D) and binding (R). Across the range of these properties and at $t_{1/2} = 0.5 \text{ h}$, maximum efficacy went from ineffective ($MxE = 0$) to completely effective ($MxE = 1$). The behavior of five representative drugs were investigated (*a*: $D = 10^{-10} \text{ m}^2/\text{s}$, $R = 10^0$; *b*: $D = 10^{-8} \text{ m}^2/\text{s}$, $R = 10^{-2}$; *c*: $D = 10^{-12} \text{ m}^2/\text{s}$, $R = 10^2$; *d*: $D = 10^{-7} \text{ m}^2/\text{s}$, $R = 10^2$; and *e*: $D = 10^{-7} \text{ m}^2/\text{s}$, $R = 10^0$). The transport properties of doxorubicin (dox) are ($D = 2 \times 10^{-11} \text{ m}^2/\text{s}$, $R = 4.8 \times 10^1$). *B)* Multiple-dose improvement (MDI) is the difference in efficacy between 20 and 1 doses. It indicates how efficacy would improve with increased doses. The measured range for MDI over all investigated drugs was $(-0.092, 0.641)$. *C)* For each drug the optimum number of doses (OpD) was determined as the minimum dose that produced at least 98% of the maximum efficacy. *D)* Drugs were arranged into five groups based on transport properties and the effect of doses on efficacy: Group I, low diffusivity; Group II, moderate diffusivity and high binding; Group III, strong binding; Group IV moderate binding; and Group V, weak binding.

Figure 6. Increased exposure throughout tissue increased efficacy. *A-D)* For a theoretical drug (**Drug D**), with half-life of 0.5 hours, diffusivity of $10^{-7} \text{ m}^2/\text{s}$ and binding constant of 10^2 , increasing overall exposure increased efficacy. *A)* With one dose, the drug concentration at the

distal edge (C_D) was initially large but quickly dropped to zero. *B*) With ten doses, C_D was smaller, but continually reappeared throughout treatment. *C*) With one dose, cell death (Fk) stopped after drug was cleared from the tissue ($Eff_{D,1} = 0.485$). *D*) After ten doses, almost all cells in the tissue are killed ($Eff_{D,10} = 0.993$). *E-F*) Normalized distal drug exposure (DDE') for all theoretical drugs after 1 (*E*) and 10 (*F*) doses. *G*) The change in distal exposure $\Delta DDE'$ matches the effect of increasing doses on efficacy (MDI ; Figure 5B).

Figure 7. Drugs retention and negative MDI . *A-D*) A theoretical drug (**Drug C**; $t_{1/2} = 0.5$ h, $D = 10^{-12}$ m²/s and $R = 10^2$) in Group II was more effective after 1 dose than after 20 doses. *A*) For **Drug C** the fraction of killed cells (Fk) was higher for 1 dose than for 20 doses throughout the treatment. *B*) The average concentration across the length of the tissue (C^{ave}) was initially greater for 1 dose compared to 20 doses. The average concentration at $T/2$ (36 h; C^{hf}) was positive and non-zero indicating that the drug had not washed out of the tissue. *C*) The concentration at the proximal edge (C_P) quickly dropped to zero after each dose, regardless of the number of doses. *D*) The concentration at the distal edge (C_D) was greater after 1 dose for most of the treatment period. *E*) Positive drug retention (Rt) indicates that the distal concentration was greater than the proximal concentration. *F*) Drugs with negative MDI values ($MDIn$) had decreased performance with more doses.

Figure 8. Effect of half-life. *A-B*) Maximum efficacy (MxE) over all treatment schedules for drugs with half-lives of 5 h (*A*) and 15 h (*B*). *C-D*) Multiple dose improvement (MDI) for drugs with half-lives of 5 h (*C*) and 15 h (*D*). *E-F*) Optimal dose (OpD) for drugs with half-lives of 5 h (*E*) and 15 h (*F*).

Figure 9. Half-life increased the concentration at the distal edge. *A)* After two doses, **Drug E** ($D = 10^{-4} \text{ m}^2/\text{s}$; $R = 10^0$), with $t_{1/2} = 0.5 \text{ h}$, appeared quickly at the distal edge and was cleared quickly. *B)* After two doses of a similar drug with the same D and R , but slower clearance ($t_{1/2} = 5 \text{ h}$), clearance from the distal region was slower. *C)* Each dose of the slow clearing ($t_{1/2} = 0.5 \text{ h}$) drug killed approximately 20% of the cells. *D)* The first dose of the slower clearing drug ($t_{1/2} = 5 \text{ h}$) killed most of the cells, so the second dose was less effective.

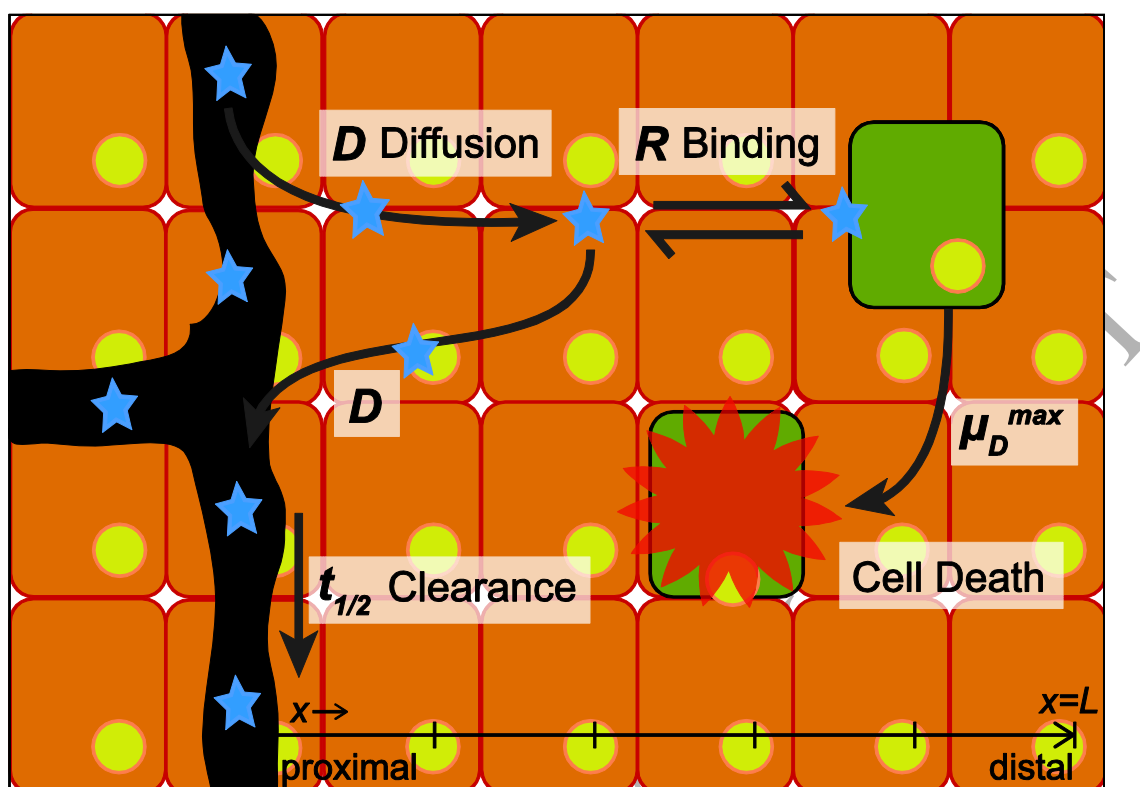


Fig. 1

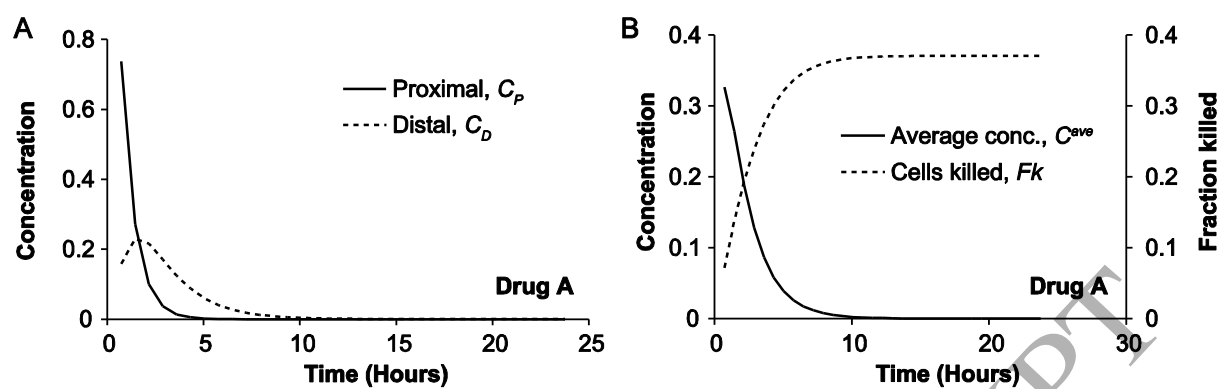


Fig. 2

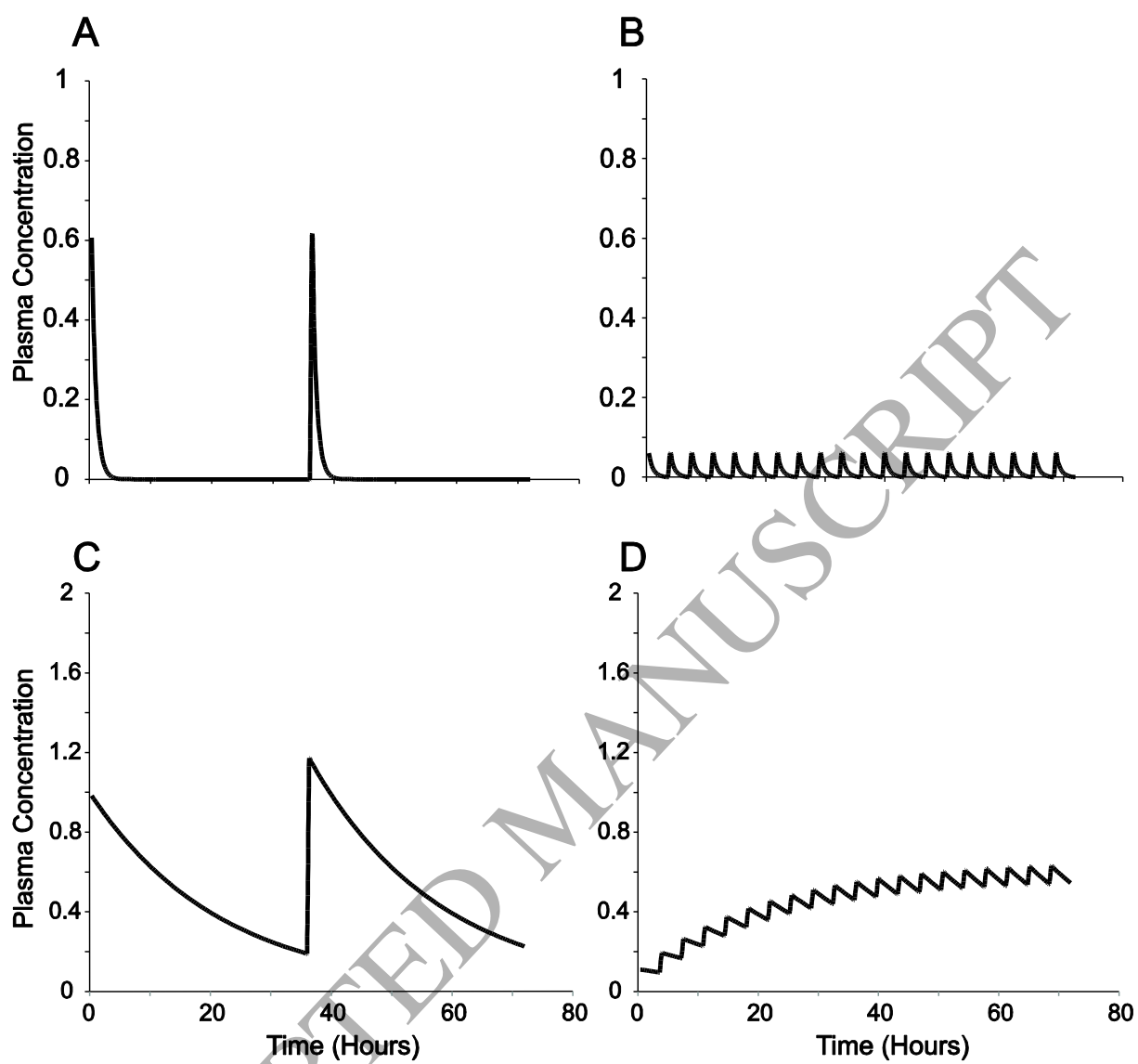


Fig. 3

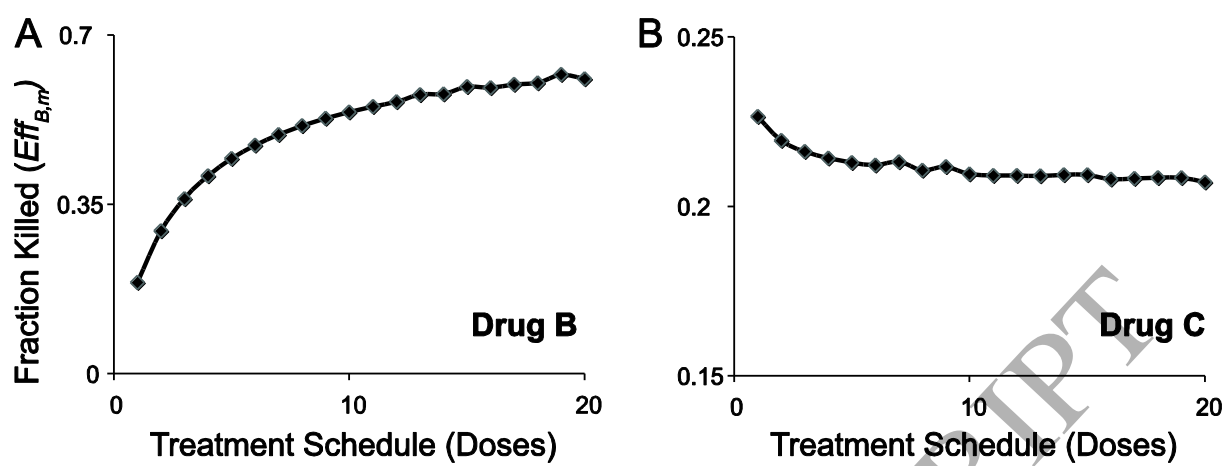


Fig. 4

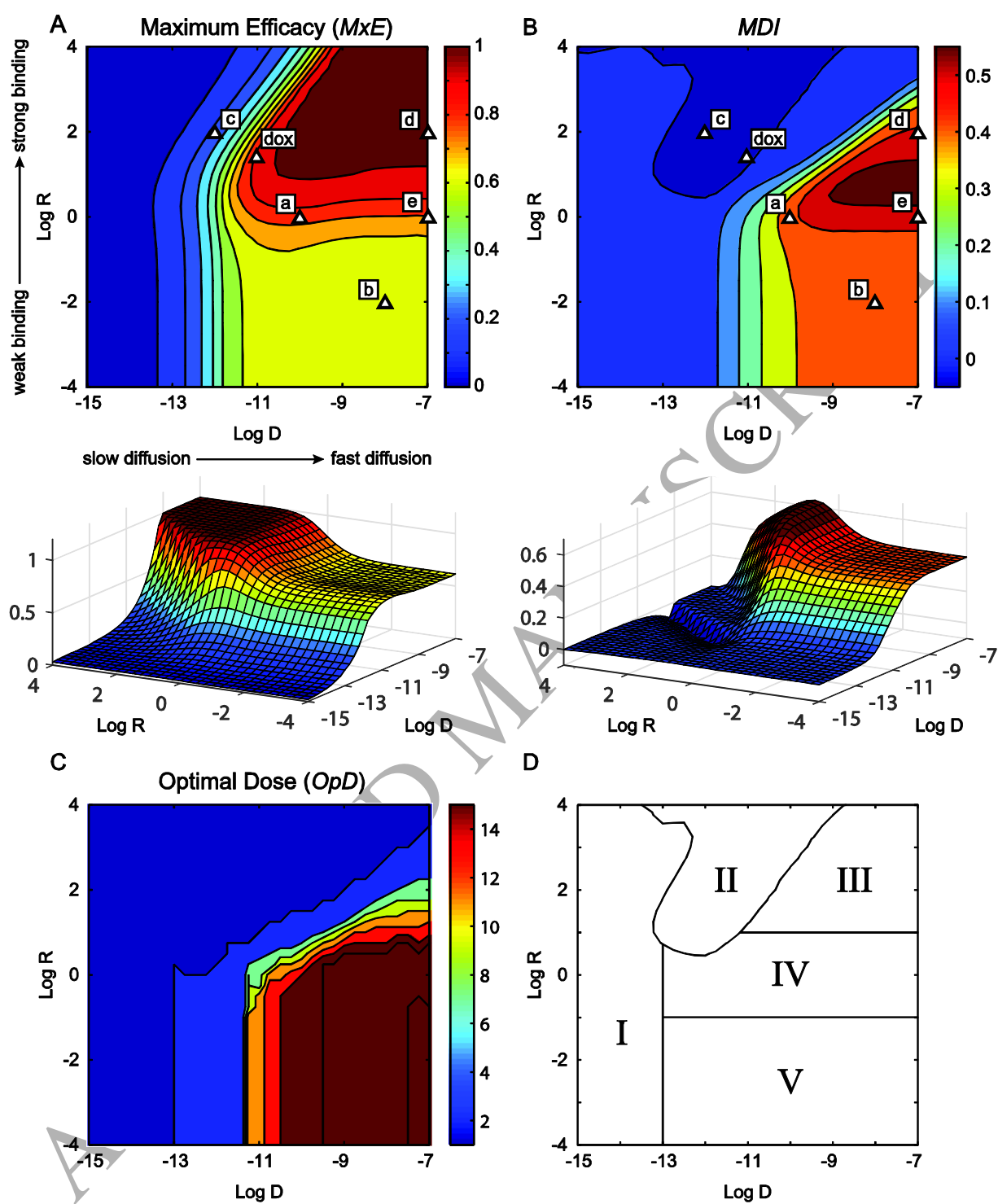


Fig. 5

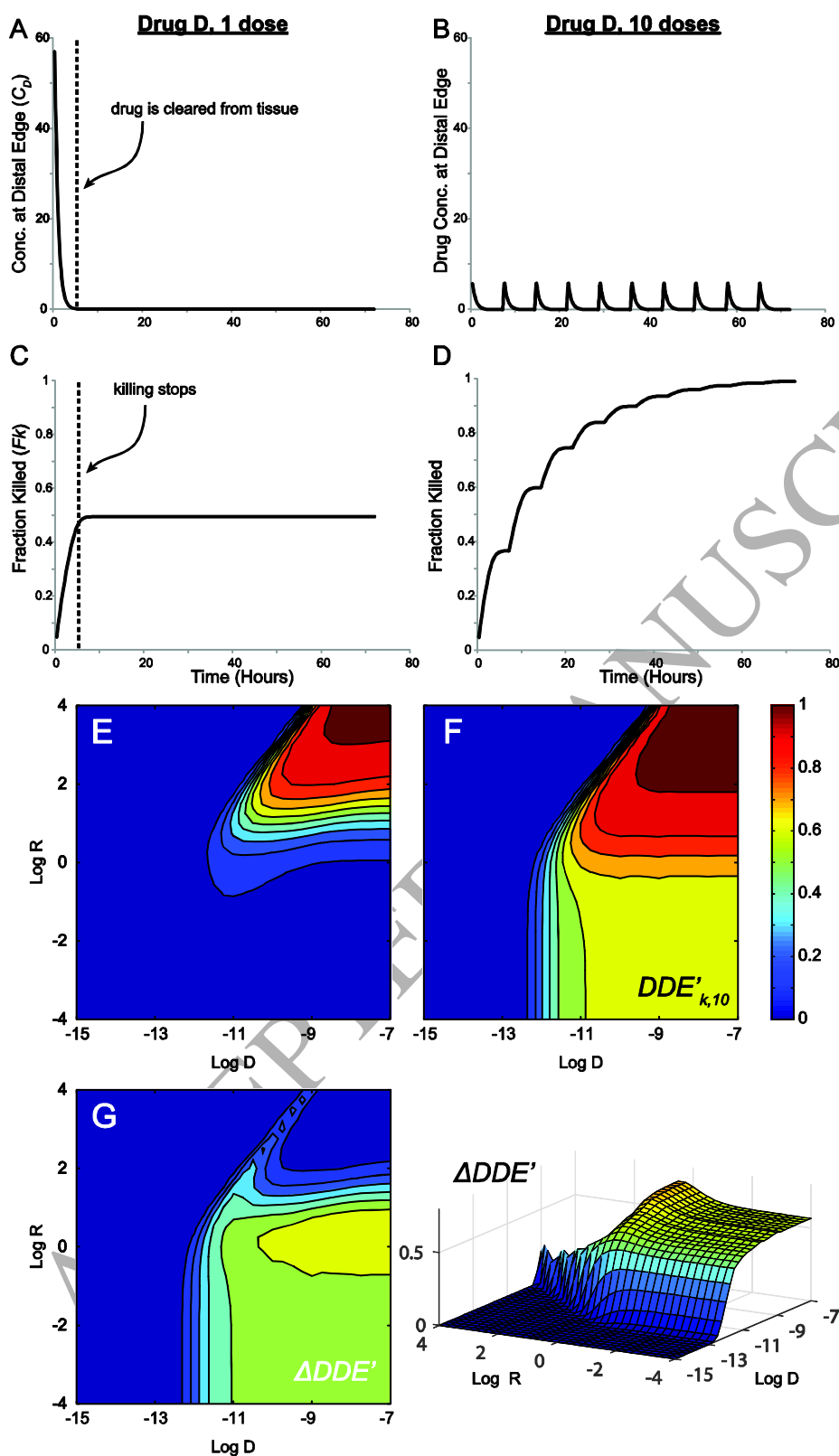


Fig. 6

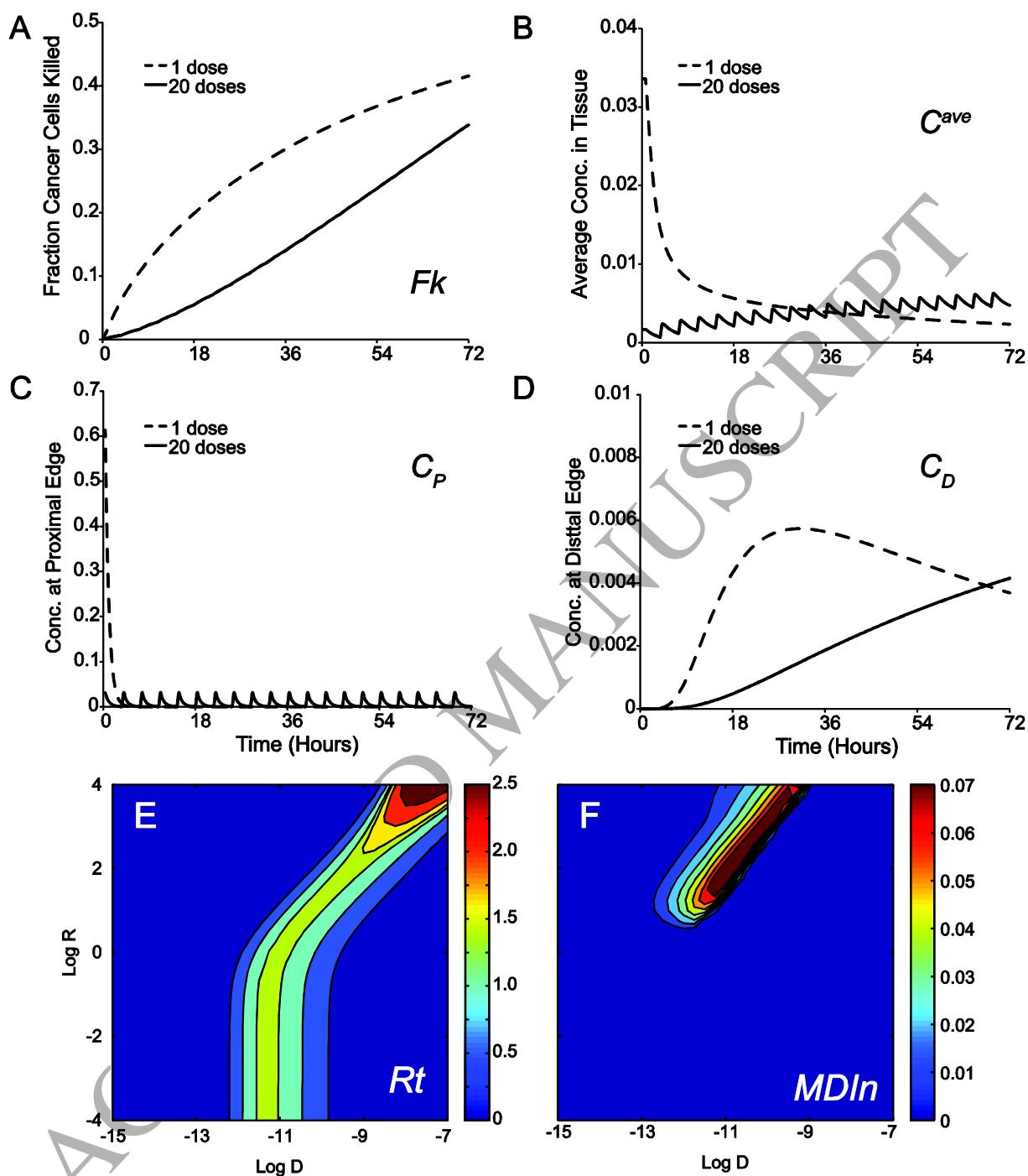


Fig. 7

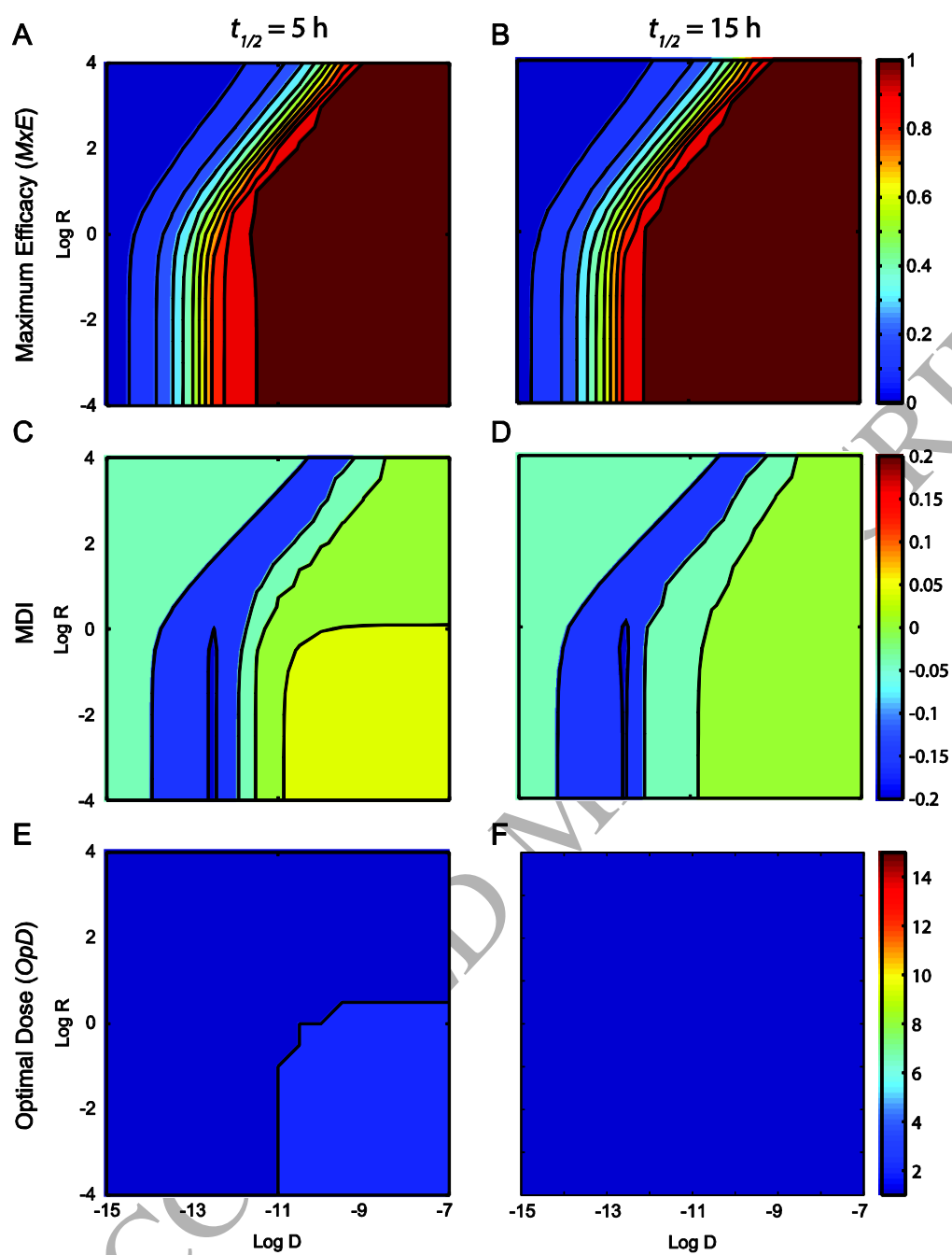


Fig. 8

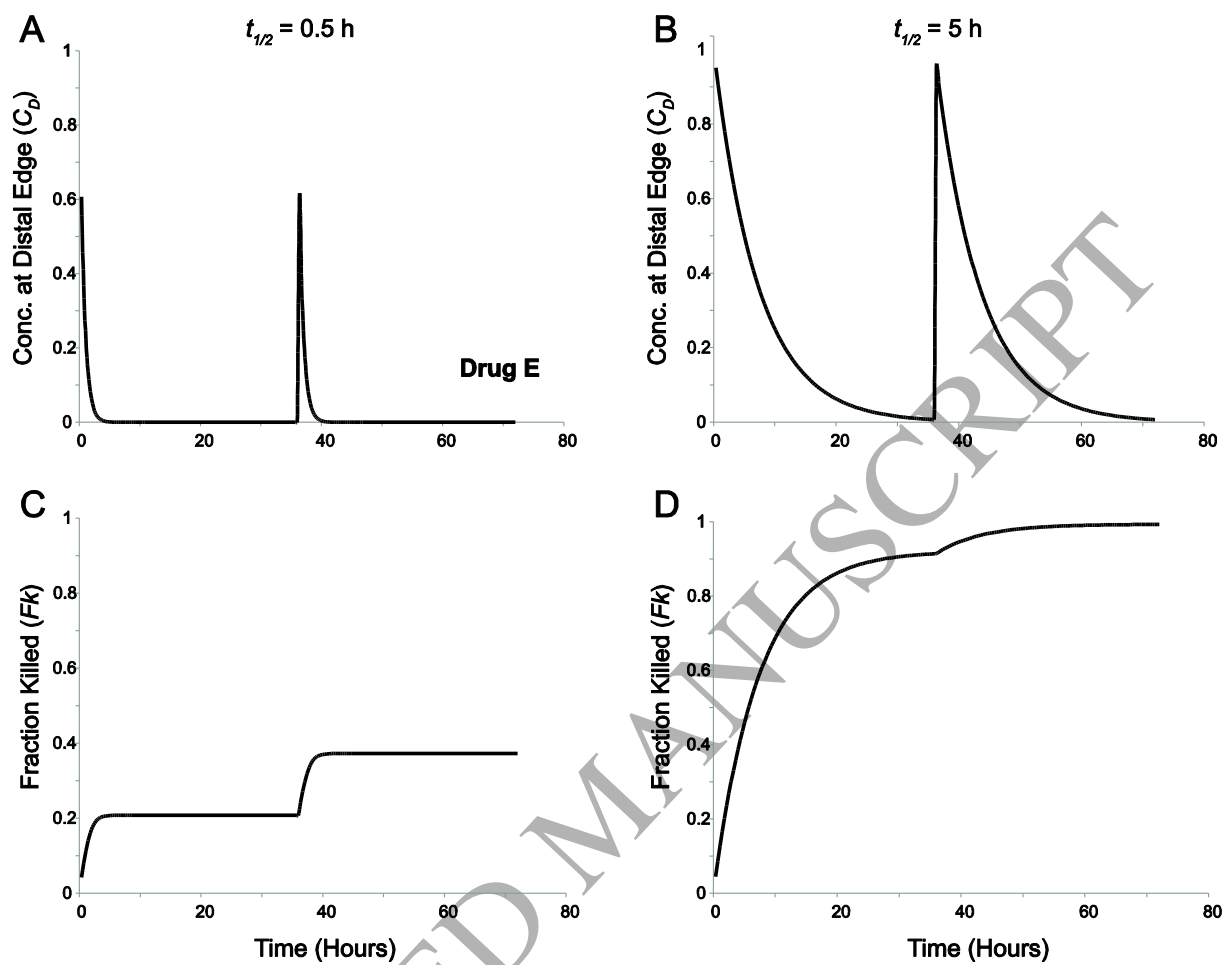


Fig. 9

Table 1. Variable (investigated) parameters for theoretical drugs

Symbol	Description	Units	Range
D	Diffusivity	$\text{m}^2\cdot\text{s}^{-1}$	10^{-18} to 10^{-2}
R ($k_{\text{on}}/k_{\text{off}}$)	Binding Constant	dimensionless	10^{-4} to 10^4
$t_{1/2}$	Clearance half-life	h	0.5, 5, 15

Table 2. Static parameters for theoretical drugs

Symbol	Description	Units	Value	Reference
L	Length	m	800×10^{-6}	(Less, Skalak, Sevic, & Jain, 1991)
C_0	Dose	$\text{mol}\cdot\text{m}^{-3}$	2×10^{-2}	(Tang et al., 2014)
K_d	Dissociation constant	$\text{mol}\cdot\text{m}^{-3}$	1.66×10^{-3}	(Toley et al., 2013)
α	Maximum rate of cell death	s^{-1}	3.89×10^{-5}	(Toley et al., 2013)

Table 3. Recommendations for treatment schedules

Diffusivity	Clearance	Cell Binding	Group	Response	Recommendation
Fast ($D < 10^{-13}$)	Fast ($t_{1/2} < 5$ h)	Strong ($R > 10^1$)	III	Always effective	Use one dose; multiple doses similarly effective
		Intermediate ($10^1 > R > 10^{-1}$)	IV	Intermediate number of doses best	Optimize for best schedule
		Weak ($R < 10^{-1}$)	V	Maximum number of doses best	Use most possible doses
	Slow ^a ($t_{1/2} > 5$ h)		II - V	Always effective	Use one dose
Intermediate ($10^{-9} > D > 10^{-13}$)	Fast ($t_{1/2} < 5$ h)	Strong ($R > 10^1$)	II	More doses reduces efficacy	Use one dose; avoid multiple doses
	Slow ($t_{1/2} > 5$ h)	All	II	More doses reduces efficacy	Use one dose; avoid multiple doses
Slow ($D < 10^{-13}$)			I	Always ineffective	Do not use

^a For drugs with intermediate clearance ($t_{1/2} = 5$ h) and weak binding (Group V), two doses was best. Optimize for best schedule.